Application Note SMX028

View on rigaku.com

SMX028 - Calibrating the XtaLAB Synergy-S for PDF analysis

Introduction

Pair Distribution Function (PDF) Analysis[1] has become a versatile tool for understanding the structure, and ultimately properties, of materials. Under normal circumstances, PDF is a technique performed using powdered samples and on suitable powder diffractometers. Modern microfocus singlecrystal diffractometers contain exceptionally bright sources and feature ultralow-noise HPC detectors that make them capable of performing high-quality diffraction experiments on microgram quantities of powder. A natural extension of these features is to perform PDF experiments on such equipment.

The most popular tool for the refinement of structures using PDF data is PDFgui[2]. In order to bootstrap refinement of a structure using PDFGui, it is important to have reasonable starting values for the unit cell parameters, and the parameters Q_{damp} and Q_{broad}. The unit cell parameters can be determined using whole powder pattern fitting (WPPF), but Q_{broad} and Q_{damp} must be determined for your experimental setup.

As a review, the data against which the atomic model is refined in PDFGui is the reduced pair distribution function, G(r). This function is the Fourier transform of Q(S(Q)-1), which is directly derived from the raw data.

Given an atomic level model, the calculated reduced PDF, $G_c(r)$, can be expressed as:

$$G_c(r) = \frac{1}{r}\sum_i \sum_j [(\frac{f_i f_j}{\langle f^2 \rangle})\delta(r - r_{ij})] - 4\pi r \rho_0$$

where $f_{i,j}$ is the scattering factor of atom i or j, ⟨f⟩ is the scattering factor averaged over all atoms in the model, r_{ij} is the distance between atoms atom i and j, and ρ_0 is the number density. The sum is over all atom pairs in the unit cell. For distances between r = 0 and the separation of the first atom pair, the function will have a slope of $-4\pi r \rho_0$. Q_{broad} is a correction for broadening from increased noise at high Q (Å^{-1}). Q_{broad} also encompasses traditional microstrain contributions from a powder sample.

Q_{broad} modifies the $G_c(r)$ peak width as shown below:

$$\sigma\prime_{ij} = \sigma_{ij}\sqrt{1 - \frac{\delta_1}{r_{ij}} - \frac{\delta_2^2}{r_{ij}^2} + Q_{broad}^2 r_i^2 j}$$

Where σ_{ij} is the peak width without correlation and is computed from the anisotropic displacement parameters. δ_1 and δ_2 account for correlated motion at different temperatures. Discussion of these two terms is outside the scope of this document. The effect of Q_{broad} is shown in Figure 1. Note how the peaks at larger values of r become broader and weaker as Q_{broad} increases.

Q_{damp} applies a Gaussian dampening envelope arising from limited Q-resolution (Å^{-1}) to the reduced PDF. Figure 2 displays the consequences of increasing Q_{damp} on G(r).

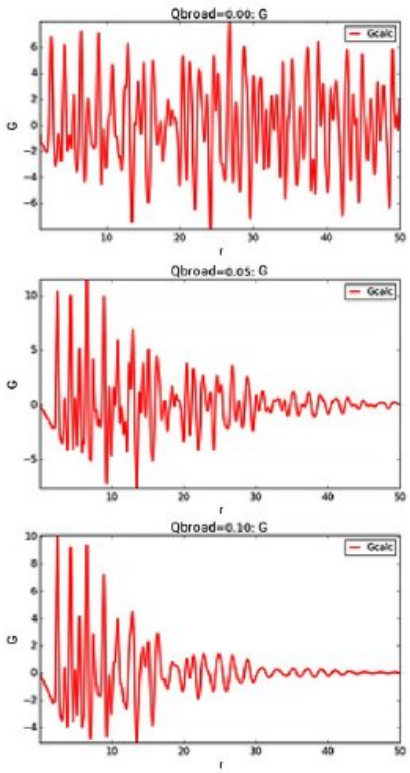

Figure 1: Effect of Q_{broad} on the calculated G(r) for nickel powder.

$$B(r) = e^{\frac{-(rQ_{damp})^2}{2}}$$

Note the effect of Q_{broad} on the reduced PDF vis-à-vis Q_{damp}. Q_{damp} causes the G(r) function to fall rapidly, but the peak widths remain the same. Q_{damp} encompasses traditional crystal size contributions from a powder sample and also allows for change in instrument peak width with change in X-ray wavelength.

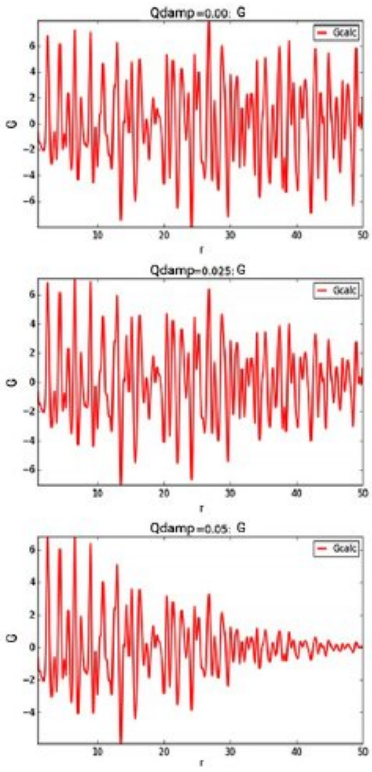

Figure 2: Effect of increasing Q_{damp} on the reduced PDF.

Experimental

For this procedure, we prepared nickel powder with a trace amount of oil in a MiTeGen³ loop as the reference standard, see Figure 3. Images for both the nickel and the background (loop and instrument) were collected on a XtaLAB Synergy-S with molybdenum radiation and a HyPix-6000HE.

The beam size at the sample is approximately 100 µm and the divergence is 4 mR. The data were collected at a sample-to-detector distance of 32 mm using a single axis scan. At this distance, a 100 µm pixel subtends an angle of approximately 0.18°. Figure 4 displays a representative diffraction image from the nickel powder sample. The images were converted to 2θ vs I data using CrysAlis^{Pro} using the appropriate Lorentz and polarization corrections. We assumed the sample was spherical around the scan axis and, thus, no absorption correction was applied.

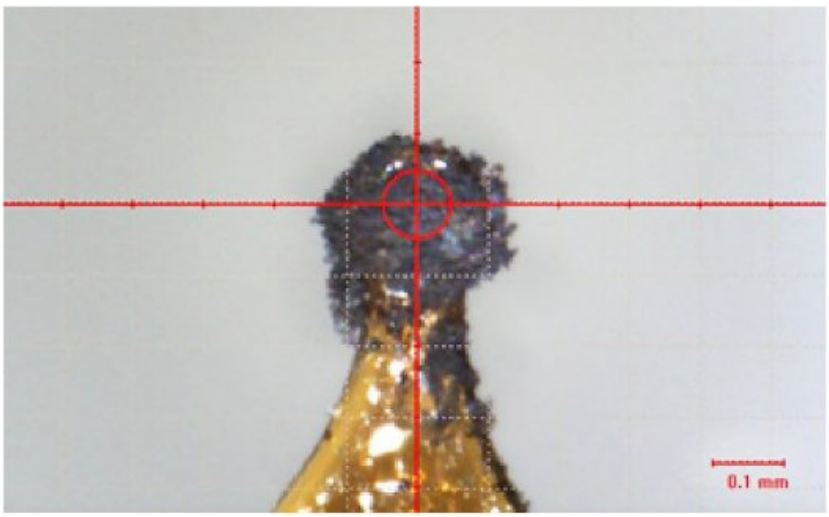

Figure 3: Nickel powder mounted on a MiTeGen loop held together with a trace of oil

The reduced G(r) was generated from the nickel and sample holder/instrument background 2θ vs I data using SmartLab Studio II using the defaults in the PDF plugin with the exception of increasing the output range from 10 Å to 50 Å.

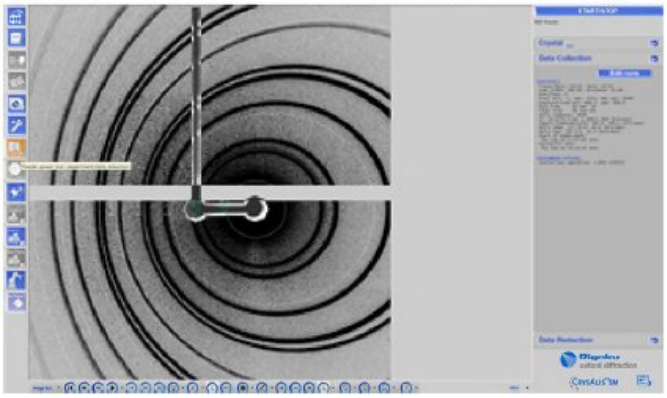

Figure 4: Representative diffraction image for nickel powder

Refinement of the model against the reduced PDF was performed with PDFGui using the CIF for Ni from the Crystallographic Open Database. In order to prevent singularities, refinement began with the scale factor and unit cell parameter, then adding the ADP, Q_{damp}, Q_{broad} and δ_2 individually until convergence one pass at a time.

The step-by-step details of the processing may be learned in the video at the Rigaku X-ray Forum.

Results

The results of the refinement are displayed in TABLE 1 and Figure 5. Figure 5 shows a good fit between the G(r) data from SmartLab Studio II (blue open circles). The refined parameters are scale factor = 1.096(13), Q_{damp} = 0.0311(6) Å, = Q_{broad} = 0.018(1) Å^{-2}, δ_2 = 1.5(2), a = b = c = 3.52457(15) Å, and U11= U22= U33 = 0.009998(18) Å^{-2} with a reduced χ^2 value of 0.124 and R_w = 0.0999.

The values of reduced χ^2 value and R_w indicate a reasonably good fit between the observed and calculated G(r) functions. Thus, the values of Q_{damp} and Q_{broad} can be used as a starting point for refinement of other similar samples measured using the same instrument configuration.

Table 1: PDFGui refinement results for nickel powder

```
DATA SET : 1 (string)

Data range in r [A]     : 1.48     -> 50          Step dr  : 0.02
Calculated range        : 1.48     -> 52.2176
Refinement r range      : 1.48     -> 50          Data pts : 0     -> 2426
Reduced chi squared     : 0.123685
Rw - value              : 0.0999149

Experimental settings   :
  Radiation             : X-Rays
  Termination at Qmax   : 17 A**-1
  DQ dampening Qdamp    : 0.0310593 (0.00062) A**-1
  DQ broadening Qbroad  : 0.0184975 (0.001) A**-1
  Scale factor          : 1.09634 (0.013)

Selected phases and atoms for this data set :
  Phase 1 :
    Atoms (i) :  NI
    Atoms (j) :  NI

Relative phase content in terms of
          atoms                    unit cells              mass
Phase 1 :1                        1                       1

PARAMETER INFORMATION :

Number of constraints         : 19
Number of refined parameters  : 6
Number of fixed parameters    : 0

Refinement parameters :
  1:1.09634 (0.013)        2:0.0310593 (0.00062)    3:0.0184975 (0.001)
 11:3.52457 (0.00015)     15:1.53429 (0.22)        24:0.00999759 (0.00018)

REFINEMENT INFORMATION:

Number of iterations : 5
Reduced chi squared  : 0.123685
Rw - value           : 0.0999149

Correlations greater than 0.8 :

  *** none ***
```

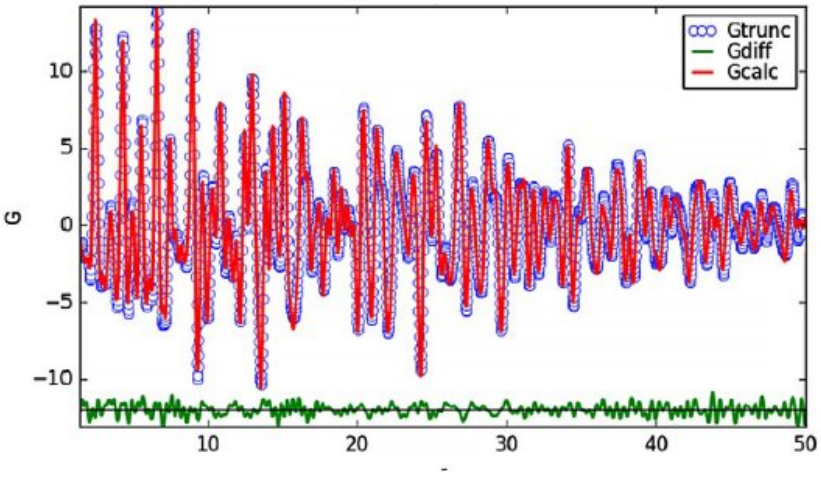

Figure 5: Observed versus calculated G(r) function. Observed data are blue circles, calculated data is the red line and the residual is the green curve

Conclusions

We have shown the process by which one can calibrate a XtaLAB Synergy system for PDF use. It is important to remember that the calibration data should be collected under the same conditions as you might collect the data on an unknown; that is, using the same wavelength, sample-to-detector distance, etc.

References

1. *Underneath the Bragg Peaks: Structural Analysis of Complex Materials*, 2nd Ed, by T. Egami and S. J. L. Billinge, Elsevier, Amsterdam, 2012.
2. PDFfit2 and PDFgui: computer programs for studying nanostructure in crystals (2007) Farrow C. L., Juhás P., Liu J. W., Bryndin D., Božin E. S., Bloch J., Proffen Th., Billinge S. J. L., *J. Phys.: Condens. Matter* **19**(33), 335219.
3. MiTeGen, LLC, P.O. Box 3867, Ithaca, NY 14852.

Related products

XtaLAB Synergy-S

Our most popular diffractometer for Chemical Crystallography and Mineralogy, configured with either single or dual microfocus sealed tube X-ray sources and an extremely low noise direct X-ray detection detector.